NACA

RESEARCH MEMORANDUM

RELATION BETWEEN FLOW RANGE AND OTHER COMPRESSOR-STAGE CHARACTERISTICS

By Arthur W. Goldstein and Ralph L. Schacht

Lewis Flight Propulsion Laboratory
Cleveland, Ohio

NATIONAL ADVISORY COMMITTEE
FOR AERONAUTICS

WASHINGTON

May 20, 1958

NACA RM E58B24

NATIONAL ADVISORY COMMITTEE FOR AERONAUTICS

RESEARCH MEMORANDUM

RELATION BETWEEN FLOW RANGE AND OTHER COMPRESSOR-STAGE CHARACTERISTICS

By Arthur W. Goldstein and Ralph L. Schacht

SUMMARY

A method based on blade-element concepts was developed to evaluate the effect of stall or choke-free angle-of-attack range on the attainable pressure rise and relative Mach numbers for cascades or single blade rows. This method was extended to evaluate the effect of usable compressor-stage flow range on the design parameters of stage flow per unit area, pressure ratio, and rotative speed. In the analysis of compressor stages, flow range (proportional to the variation of the ratio of flow at positive stall to flow at choke or negative stall from 1.0) was taken as the independent variable, and the effect of range on these design parameters was evaluated. The analysis indicates that high inlet Mach number designs necessarily have small flow ranges and that blade rows with maximum flow ranges are designed for choked-discharge flow. The greatest flow range is attained at low values of Mach number, flow per unit area, and over-all diffusion, and at high surface-velocity diffusion. Blades designed to attain large surface-velocity diffusion may be used for either large pressure ratios or large flow ranges.

INTRODUCTION

Compressor design procedure is normally concerned with a single operating point, and all stages are designed to satisfy requirements at this condition. In practice, however, off-design operation often proves to be the decisive factor in the evaluation of compressor suitability. Therefore, compromises in stage capabilities are generally made in order to obtain better off-design performance. For example, in a compressor of many stages, the front and rear stages operate over a wide range of flow coefficients as speed and pressure ratios are varied. In multistage designs, the flow capacity (flow per unit frontal area) or pressure ratio is normally reduced from the maximum attainable in order to achieve improved ranges of stall or choke-free operation for the front stages and thus minimize off-design operating problems.

In order to make effective design compromises to ensure adequate off-design compressor performance, additional knowledge of the relation between usable stage flow range and such design parameters as flow per unit frontal area, stage pressure ratio, and rotative speed is required. A reasonable approximation to the relations of the primary variables (choke-flow coefficient, stall-flow coefficient, relative flow angle, and area contraction) is made, and these approximations are used to estimate the relations between stage flow range and the compressor-stage performance parameters (flow per unit area, stage pressure ratio, rotative speed, etc.). From this, the following information will be sought: What combinations of compressor characteristics are obtainable, which characteristics must be sacrificed to improve a desired operation mode, and upon which blade-row qualities research and development should be concentrated.

Inasmuch as generalized angle-of-attack limits are not readily defined for any arbitrary blade section, a particular section considered applicable to high-performance compressors was selected, and operating limits were estimated from basic flow theory. Although the results were obtained for a particular type of blade shape, the trends are believed to be generally applicable to the type of blade sections currently in use.

In the analysis, the blade row is treated as a two-dimensional cascade. The operating limits of a cascade or a blade row are first estimated and then extended to a stage. Stage flow range is then taken as the independent variable; and other operating characteristics, such as choke-flow limit, pressure ratio, and operating speeds, are defined for selected values of flow range.

SELECTION OF BLADE SECTIONS

Because the operating conditions assume high-performance compressors and, therefore, high subsonic Mach numbers, the wedge-shaped leading edge is considered appropriate; blades of this type have low surface velocities and less danger of local shocks than blunt-nose types suitable for large range at low subsonic velocities. Also appropriate for blades of this type are gradual curvatures that help keep local velocities low. In a later section of the report, the highest local velocity required is shown to be a minimum when the surface velocity is constant on the suction surface over the anterior exposed region between the leading edge and the point (A) found by dropping a perpendicular from one leading edge to the suction surface of the adjacent blade (fig. 1). This perpendicular marks the entrance to the channel between blades. In reference 1, a calculated example for a cascade of thin circular arcs shows that such a nearly constant surface velocity is obtained. Consequently, the suction surface of the proposed blades may be expected to resemble circular-

arc sections in the exposed part upstream of the channel entrance, since this surface will have nearly constant curvature.

If the cascade is to operate at high flows, constricting the flow channel between blades and thus forming an internal throat smaller than that required at the entrance to the channel between blades is inappropriate. Consequently, the direction of the pressure surface of the blade section near the leading edge will be parallel to the opposite suction surface (point A of fig. 1) if the leading-edge wedge angle is to be a maximum. For a blade row with maximum flow range the use of a maximum wedge angle at the leading edge is desirable; this assumption is discussed later in the report.

To summarize the blade-row characteristics, the blade sections discussed in this report have the following properties: (1) The leading edges will be wedge-shaped except for a small radius of curvature required for fabrication; (2) the anterior part of the suction surface between the leading edge and the entrance of the channel between blades will not deviate strongly from a circular arc, since this part must have nearly constant curvature in order to maintain a near constant surface velocity at stalling inflow conditions; (3) the entrance to the interblade channel will have parallel walls; and (4) the other geometric features of the blade are not specified but are assumed appropriate to achieve what are regarded as attainable performance properties. The chord, for example, is not specified nor is any portion of the pressure surface other than the angle at the leading edge. Typical limitations on the shape are: (1) An internal throat must not be formed, and (2) the surface velocity must not rise to a value higher than that on the anterior exposed part of the suction surface.

FLOW RANGE OF CASCADES

Now that the principal shape factors of the blade sections have been specified, the effective or useful range of angle of attack for the operation of these shapes must be determined. At large positive or negative angles of attack, the flow separates from the surface. This condition of stall is accompanied by large losses. Thus, the useful range of inflow angles is limited by the occurrence of positive or negative stall. In many cases the stall is gradual, and this indefinite characteristic has led to several definitions of stalling limit for compressor-blade rows, such as (1) positive angle of attack with maximum pressure rise, (2) positive angle of attack for maximum deflection, (3) angle of attack for separation of the boundary layer, (4) angle of attack with loss coefficient twice the minimum value, and (5) angle of attack when the flow is unstable and flow pulses travel from one blade to another (rotating stall). In the present analysis, only stall limits (3) and (4) are considered.

[redacted]

At high airspeeds, another limit takes precedence over the condition of negative stall - this is the condition of choke. With Mach number equal to 1.0 in the blade-passage throat, further decreases in back pressure will not change the upstream flow but will merely increase losses.

Blade Stall

Data from isolated airfoils examined in reference 2 show that a good correlation of flow separation is obtained with the ratio of maximum surface velocity to free-stream velocity. That is, within reasonable limits on the velocity distribution, the velocity distribution is of secondary importance compared with the over-all velocity change. The critical velocity ratio was found to be 2.3. The data of references 3 and 4 on cascades of low-speed airfoils are examined in reference 5; and it is shown that, when the ratio of maximum surface velocity to discharge velocity is 1.83, the losses begin to increase and that, when a ratio of 2.0 to 2.2 is attained, the losses are doubled. Unlike the isolated airfoil, the stall limit in cascades is clearly influenced by the over-all velocity decrease for the cascades as well as the angle of attack that affects the maximum surface velocity near the leading edge. Theoretically, almost any velocity ratio may be used, but large velocity ratios require long chords and are critical in pressure distribution. A ratio of 1.85 to 2.0 may be attained with reasonably long chords and is not critically dependent on details of the blade shape or inflow state of the gas.

For sharp-edged airfoils, the surface velocity is always large enough to ensure separation at all angles other than the angle for smooth inflow. This smooth inflow angle is somewhat less than the camber-line direction near the leading edge. The boundary layer subsequently reattaches to the airfoil, and diffusion is begun with a boundary layer less able to withstand diffusion than in the case of the round-nosed airfoil. The higher the incidence angle, the worse the boundary-layer condition. Consequently, the ratio of the surface velocity to the discharge velocity that may be used without blade stall is a function of the incidence angle for which the blades are designed. In selecting values of the incidence angle for stall, experimental data should be used for shapes approximately of the type being considered. The double-circular-arc blades are therefore appropriate, and the data of references 6 and 7 (replotted in fig. 2) show that, for negative incidence angles, an inflow direction parallel to the pressure surface gives approximately twice the lowest loss and is in a region of rapidly rising loss with angle change. Analogously, the loss might be expected to show a similar limit when the inflow is parallel to the suction surface, since the phenomenon of separation and reattachment is local to the leading-edge region. If such a limit is selected, the discharge velocity that may be attained for that angle must next be estimated. On both the curves shown, the losses rise to very large values, since diffusion stall has occurred at a lower angle

because of the high values of suction-surface diffusion. For the condition of flow parallel to the suction surface, the ratios of average velocity on the surface upstream of the channel entrance to the downstream velocity are 2.4 and 2.5 for the tests of references 7 and 6, respectively. No other data on double-circular-arc cascades are available.

Thus, the lower limit of angle of attack may be either negative stall (angle less than the angle tangent to the pressure surface) or choke. The upper limit of angle of attack may be either positive stall (angle greater than the angle tangent to the suction surface) or excessive surface-velocity diffusion. At low inflow Mach numbers, the incidence angle will be the limit. At high inflow Mach numbers, choke and surface-velocity-diffusion stall will limit the range. Figure 3 shows these general limits and is discussed in detail in a later section.

Estimate of Maximum Surface Velocity

In a plane section of a blade row of the type being considered, a potential line may be drawn from the leading edge of one blade to the suction surface of the next (BA in fig. 1). This defines the suction-surface length b. The circulation theorem gives

$$sV_1 \sin \theta_1 = \int_0^b v \, dx = b\bar{v} \qquad (1)$$

where θ_1 is the inflow angle and $\bar{v}$ is the average velocity on the anterior blade length b. (All symbols are defined in appendix A.)

For a given blade geometry, the length b will depend only slightly on θ_1 if the solidity of the blade row is sufficiently high, since the flow pattern in the interblade channel will change only slightly with inflow angle. Since the channel walls are parallel at the entrance, the potential line is approximated as a straight line from the leading edge that is normal to the suction surface at the point of intersection. The maximum surface velocity v_m can be kept to a minimum value for a fixed average value when v is constant over the region b. In this case, $v_m = \bar{v}$. If $1/\bar{R}$ is the average curvature on the length b, then using the circular-arc approximation results in $b = \bar{R}(\beta_s - \beta_p)$, and

$$\bar{R}/s = \frac{\sin \beta_p}{\sin(\beta_s - \beta_p)} \qquad (2)$$

Substitution yields

$$\frac{\bar{v}}{V_1} = \frac{s \sin \theta_1}{\overline{R}(\beta_s - \beta_p)} = \frac{\sin \theta_1}{\sin \beta_p} \frac{\sin(\beta_s - \beta_p)}{\beta_s - \beta_p} \tag{3}$$

For small angle differences, $\beta_s - \beta_p \approx \sin(\beta_s - \beta_p)$,

$$\frac{\bar{v}}{V_1} = \frac{\sin \theta_1}{\sin \beta_p} \tag{4}$$

where θ_1 is the inflow angle for which v is constant on b. The velocity ratio v_m/V_2 that can be used to determine a stalling value for V_2 is then

$$\frac{v_m}{V_2} = \frac{V_1}{V_2} \frac{\sin \theta_1}{\sin \beta_p} \tag{5}$$

As previously mentioned, the θ_1 value of interest is $\theta_1 = \beta_s$. In this case the formula gives an average surface velocity

$$\frac{\bar{v}}{V_2} = \frac{V_1}{V_2} \frac{\sin \beta_s}{\sin \beta_p} \tag{6}$$

which may be used in place of v_m/V_2 if the empirical value is based on $\bar{v}/V_2$.

The only fact presently known is that the average velocity ratio should be somewhat less than 2.0. In the present analysis, values of 1.75 and 1.55 are investigated because these values should be obtainable without critical blade-design requirements and should allow somewhat for the effect of the sharp leading edge on the condition of the boundary layer.

Equation (6) relates the operating range of angles to the over-all velocity change after an appropriate value of the average velocity $\bar{v}/V_2$ is selected. This relation is independent of design details and relates only operational variables.

Choking Limits of Cascade Operation

If the back pressure on a cascade is reduced, the inflow Mach number will increase until the velocity in the channel throat is

approximately sonic. If there is a velocity variation across the throat, the choking or maximum inflow is given by

$$\left(\frac{\rho_1 V_1}{\rho^* a^*}\right)_c = \frac{1 - 0.4\Delta M^2}{\cos \theta_{1,c}} \frac{\cos\left(\frac{\beta_s + \beta_p}{2}\right)}{\cos\left(\frac{\beta_s - \beta_p}{2}\right)} \tag{7}$$

where

$$\Delta M = \frac{M_A^* - M_B^*}{M_A^* + M_B^*} \cong \frac{1}{2}\left(\frac{\sin \beta_s}{\sin \beta_p} - 1\right)$$

This result is derived in appendix B and determines the inflow Mach number as a function of the inflow angle θ_1 for $\theta_1 < (\beta_s + \beta_p)/2$. The accuracy for determining Mach number from $\rho_1 V_1/\rho^* a^*$ is not good if the Mach number is near 1.0; the equation will be more satisfactory as an indicator of maximum flow rather than of choking Mach number. The flow limit in blade rings of variable section will be somewhat less when the spanwise variations do not permit simultaneous choke of all sections, but this situation does not affect the estimate of obtainable flows for compressor stages that are here assumed to be designed for maximum flow. The flow limits are regarded as applicable to unswept blades only, since spanwise flow may extend the range of swept blades.

OPERATING CHARACTERISTICS OF SINGLE BLADE ROWS

Up to this point, the low-speed flow-angle limits for β_s and β_p have been related to the over-all velocity ratio V_2/V_1 at stall and to the maximum flow rate. The surface diffusion will increase with increasing inlet Mach number as an effect of compressibility where the operating speed is increased over that at which the stalling velocity ratio V_2/V_1 is designed to occur for $\theta_1 = \beta_s$, and stalling will occur unless θ_1 is decreased to a value less than β_s. The choke limit will require a larger angle with increased inlet Mach number so that eventually, at some speed, choke and stall will occur simultaneously unless shock losses are sufficient to provide an operation limit before this Mach number is attained. The blade-row limit curve will have the general appearance shown in figure 3.

The placement of the lines for β_s and β_p (inflow angles parallel to the suction and pressure surfaces, respectively) determines the inlet leading-edge wedge shape and the size of the throat section for the blade

sections previously characterized in this report. Therefore, β_s and β_p determine the location of the choke curve or, alternatively, the entire choke curve is specified by a single point on it. The stall curve is as yet unspecified since the point at M_s, β_s (fig. 3) can be freely assigned; in a compressor, the value of M_s is chosen to occur at the same wheel speed as the choke flow at M_c. Once this point (M_s,β_s) is chosen, the value of the discharge Mach number is determined from the velocity ratio V_2/V_1. The equation of continuity with the abbreviation $g \equiv \rho V/\rho^* a^*$ states that for any inflow condition g_1,θ_1 and for choking inflow condition $g_{1,c}\theta_{1,c}$

$$g_2 A_2 \cos \theta_2 = g_1 A_1 \cos \theta_1$$

$$g_{2,c} A_2 \cos \theta_{2,c} = g_{1,c} A_1 \cos \theta_{1,c}$$

where A_1, A_2 are the frontal areas of the cascade at entrance and exhaust. If negligible variation of the discharge angle θ_2 is assumed and if choke occurs at maximum range of $\theta_{1,c} = \beta_{1,p}$,

$$\frac{g_2/g_1}{(g_2/g_1)_c} = \frac{\cos \theta_1}{\cos \theta_{1,c}} = \frac{\cos \theta_1}{\cos \beta_{1,p}} \tag{8}$$

Since the flow density ratio g_2/g_1 can serve as a measure of cascade diffusion, the increase of diffusion as θ_1 increases from $\beta_{1,p}$ to $\beta_{1,s}$ is indicated.

For low inlet Mach number, $\cos \beta_{1,s}/\cos \beta_{1,p}$ is an indication of flow range; values close to 1.0 indicate $\beta_{1,s}$ close to $\beta_{1,p}$ and small range, whereas small values of $\cos \beta_{1,s}/\cos \beta_{1,p}$ indicate large range.

A single chart may be used with these interpretations to describe to a large degree the performance characteristics of blade rows by utilizing the relations of equations (7) and (8). Such a chart is shown in figure 4, where the range parameter $\cos \beta_{1,s}/\cos \beta_{1,c}$ is plotted against the ratio of cascade-flow capacity to the annulus choke-flow capacity $(g_1 \cos \beta_1)_c$ with contours of inlet choke-flow Mach number and angle and over-all diffusion $D \equiv \dfrac{\sin \beta_c}{\sin \beta_s} = \dfrac{V_{1,s}}{V_{2,s}}\left(\dfrac{V_2}{\bar{v}}\right)_s$. Over-all diffusion was used to make the chart general since $D\left(\dfrac{\bar{v}}{V_2}\right)_s = \left(\dfrac{V_1}{V_2}\right)_s$, and the

one chart can then be used for any value of $\overline{v}/V_2$ chosen. Blockage due to blade thickness has not been accounted for on this figure.

The cascades to which this chart is applicable are those previously described, where the choke inflow Mach number is the highest at which the inflow angle may be as low as β_c (fig. 3), the intersection of the choke line and the negative stall line, $\theta_{1,c} = \theta_{1,p}$.

This point may be regarded as the design condition. The positive stall condition is also assumed to occur at the maximum Mach number at which the inflow angle $\theta_{1,s}$ is equal to $\beta_{1,s}$, so that diffusion stall and leading-edge stall occur simultaneously. Actually, the flow range is the maximum attainable and is proportional to the variation of $\cos \beta_{1,s}/\cos \beta_{1,p}$ from 1.0, where the range is clearly zero. The entire range of design parameters indicated by figure 4 is not usable because the flow at choke is limited by the possibility of choking at the discharge ($g_{2,c} = 1.0$). The continuity equation (8) then reduces to

$$\frac{V_{2,s}}{a^*}\frac{\rho_{2,s}}{\rho^*} = g_{2,s} = \frac{g_{1,s}\cos\beta_{1,s}}{g_{1,c}\cos\beta_{1,p}} \tag{9}$$

The stall condition (eq. (6)) also describes the exit velocity $V_{2,s}$:

$$\frac{V_{2,s}}{a^*} = \frac{V_{1,s}}{a^*}\frac{\sin\beta_{1,s}}{\sin\beta_{1,p}}\left(\frac{V_2}{\overline{v}}\right)_s = \left[\frac{V_{1,s}}{V_{1,c}}\frac{\sin\beta_{1,s}}{\sin\beta_{1,p}}\left(\frac{V_2}{\overline{v}}\right)_s\right]\frac{V_{1,c}}{a^*} \tag{10}$$

Because $g = \frac{V}{a^*}\left[1 + \frac{\gamma - 1}{2}\left(1 - \frac{V_2^2}{a^{2*}}\right)\right]^{\frac{1}{\gamma-1}}$ the discharge velocity $V_{2,s}/a^*$ may be eliminated between equations (9) and (10) if a value for the diffusion ratio $(\overline{v}/V_2)_s$ is assumed and a relation is obtained between stall and choke inflow for this cascade design limit of $M_{2,s} = 1.0$. However, the velocity ratio $V_{1,s}/V_{1,c}$ may still be chosen at will. The exit-choke line for $(\overline{v}/V_2)_s = 1.75$ is shown in figure 4 for the case of $V_{1,c} = V_{1,s}$ and $g_{1,s} = g_{1,c}$. This single curve was obtained from equations (9) and (10) and the approximation $g \cong 1 - \frac{\gamma - 1}{2}(1 - M)^2$. All designs must be above and to the left of this curve if the inlet stall and choke Mach numbers are equal.

[redacted]

The chart (fig. 4) shows that, as the choke Mach number increases, the range factor approaches 1.0; that is, the range is small. For example, at $M_{1,c} = 0.9$ the range factor is 0.98 and, therefore, the cosine of the inflow angle may vary only 2 percent between $\cos \beta_{1,c}$ and $\cos \beta_{1,p}$. At $M_{1,c} = 0.7$, $\cos \beta_{1,s}/\cos \beta_{1,c} = 0.82$, so that an 18-percent variation is permitted. Further, the exit-choke line indicates that large range is obtained only at low flows. For example, at a flow density of $g_{1,c} \cos \beta_{1,c} = 0.8$ of the annulus capacity, the range factor may be as low as 0.82, so that an 18-percent variation is the maximum possible; whereas, at $g_{1,c} \cos \beta_{1,c} = 0.4$, the maximum range possible is 50.6 percent, since at exit choke the cosine ratio is 0.494. At the same time, $\cos \beta_{1,c}$ is reduced from 0.88 ($\beta_{1,c} = 28.4^\circ$) to 0.525 ($\beta_{1,c} = 58.33^\circ$). If a surface diffusion ratio $(\overline{v}/V_2)_s$ greater than 1.75 were used, the exit-choke curve would be lowered and would permit larger flow range. For any fixed Mach number or flow range $\cos \beta_{1,s}/\cos \beta_{1,p}$, the largest diffusion is obtained at the lowest flows, as indicated by the larger values of D on the left side of the chart. At high flows (right side of chart), large values of diffusion are obtained only at small range $\cos \beta_{1,s}/\cos \beta_{1,p}$ near 1.0 or at large Mach numbers. Compressor stages of high flow would have to be designed in this region and, thus, would have small flow-range capacities.

4208

CHARACTERISTICS OF COMPLETE COMPRESSOR STAGE

Calculations

The blade-row analysis can be applied to estimate the characteristics of a complete stage, which consists of a rotor and a downstream stator. In the analysis of the blade row, it was unnecessary to specify the value of the discharge velocity at stall or choke or to state the discharge angle or span variation in passing through the blade row. Since this now must be done in order to find the performance of the combination, a stall value must be assumed for the velocity diffusion ratio $(\overline{v}/V_2)_s$. A value of $(\overline{v}/V_2)_s = 1.75$ is assumed as usable, but a value of 1.55 is also used in the calculations in order to obtain some estimate of the effect of this variable. Also, the flow relative discharge angle from the stator and from the rotor is assumed constant regardless of the inflow conditions. This condition relates the gas velocity at choke and stall by

$$\tan \beta_1 = \tan \beta'_{1,s} - \frac{1}{\varphi_{1,s}} = \tan \beta'_{1,c} - \frac{1}{\varphi_{1,c}} \qquad (11)$$

where β is the (constant) absolute angle of discharge from an inlet guide vane, β' is the flow angle relative to the rotor, and the flow coefficient $\varphi = V \cos \beta / U = W \cos \beta' / U$ (wherein W_1 is the relative velocity, V_1 is the absolute velocity, and U is the linear speed of the rotor). Similarly,

$$\tan \beta_2' = \tan \beta_{2,s} + \frac{1}{\varphi_{2,s}} = \tan \beta_{2,c} + \frac{1}{\varphi_{2,c}} \tag{12}$$

is regarded as constant.

If the flow coefficients $\varphi_{1,c}$ and $\varphi_{1,s}$ and the choke angle $\beta_{1,c}'$ are assumed, then in turn the following may be calculated:

(1) Inlet-guide-vane discharge angle from $\tan \beta_1 = \tan \beta_{1,c}' - \frac{1}{\varphi_{1,c}}$

(2) Relative inflow angle at stall from $\tan \beta_1 = \tan \beta_{1,s}' - \frac{1}{\varphi_{1,s}}$

(3) Relative inflow Mach number $(W_1/a_1)_c$ at choke from equation (7) (modified to rotor-flow notation)

(4) Over-all relative velocity ratio $(W_2/W_1)_s$ from stall-condition equation $\left(\frac{W_1}{W_2}\right)_s \left(\frac{\overline{w}}{W_2}\right)_s \frac{\sin \beta_{1,c}'}{\sin \beta_{1,s}'}$ and rotor speed U_1/a_a from $\varphi_{1,c}$ and $\left(\frac{W_1}{a_a} \cos \beta_1'\right)_c$

The rotor-discharge flow area is then

$$\frac{h_2}{h_1} \cos \beta_2' = \left(\frac{G_1}{G_2} \cos \beta_1'\right)_s = \left(\frac{G_1}{G_2} \cos \beta_1'\right)_c$$

where h is the annulus area per blade channel. Then the discharge Mach number at choke flow $(W_2/a_2)_c$ can be determined from $G_{2,c}$. At this point it is necessary to assume either h_2/h_1 or $\cos \beta_2'$ in order to continue the problem. When h_2/h_1 is assumed, $\beta_{2,c}$, $\beta_{2,s}$, and the flow densities of the absolute flow may be calculated:

$$g_{2,c} = \left(\frac{\rho_2 V_2}{\rho_2^* a_2^*}\right)_c \quad \text{and} \quad g_{2,s} = \left(\frac{\rho_2 V_2}{\rho_2^* a_2^*}\right)_s$$

The velocity $V_{3,s}$ may be determined as well as the discharge area $(h_3 \cos \beta_3)/h_1$ and the exit-choke velocity $V_{3,c}$. Also, the flow density in the stator throat $g_{2,T,c}$ is required at the choke flow. From these data the work output or other derived data may be found.

Accordingly, four independent variables, such as $\varphi_{1,c}$, $\varphi_{1,s}$, $\beta'_{1,c}$, and β'_2, must be assumed in order to completely solve for the stall and choke values of flow, pressure ratio, and discharge Mach number as well as the compressor tip speed. This speed is the highest for which the full range (stall and choke at relative angles $\beta'_{1,s}$ and $\beta'_{1,c}$, respectively) can be utilized. At higher tip speeds, the stall and choke angles approach each other (fig. 3), and maximum flow range cannot be achieved.

Limits of Compressor-Stage Design

Not all assumed values of the four input variables lead to physically possible designs. Auxiliary conditions that must be satisfied are subcritical flow density out of the rotor ($G_{2,c} < 1$), in the stator throat ($g_{2,T,c} < 1$), and out of the stator ($g_{3,c} < 1$). A large number of designs were computed with surface-velocity-diffusion ratios of $(\overline{v}/V_2)_s = 1.75$ and 1.55 for each of the three channel angles $\beta'_{1,c} = 30^\circ$, 45°, and 60°; in no case did rotor-exit choke ($G_{2,c} = 1$) provide a limit, since the stator always choked first. The three parameters of $\beta'_{1,c}$, $\varphi_{1,c}$, and $\varphi_{1,s}$ completely determine the conditions of flow into the rotor and the relative discharge velocities $W_{2,s}$, $W_{2,c}$, but leave free the choice of the blade annulus area at discharge. If the rotor-outlet annulus area is reduced, thus reducing h_2/h_1, the continuity condition requires that the discharge angle β'_2 approach zero and thus increase the work output of the rotor and the Mach number into the stator. The minimum value of h_2/h_1 is reached when the stator throat is choked ($g_{2,T,c} = 1.0$).

In all the calculations made, the design point was taken as the choke-flow point that is considered to be the normal or design operating condition for an inlet stage. An inlet radius ratio of 0.5 and a constant tip radius were also assumed.

Figure 5(a) shows typical results of the calculations for the design point at $\varphi_{1,c} = 0.65$, $\beta'_{1,c} = 45^\circ$ for various values of $\varphi_{1,s}$ and h_2/h_1. The surface-velocity ratio $(\overline{v}/V_{2,3})_s$ was taken as 1.75. The

range of possible designs for $h_2/h_1 = 1.0$ is from $\varphi_{1,s}/\varphi_{1,c} = 1.0$ ($g_{2,T,c} = 1.0$) to $\varphi_{1,s}/\varphi_{1,c} = 0.752$ ($g_{3,c} = 1.0$). As h_2/h_1 is decreased, this range of possible designs would be reduced until the stator throat and discharge both choked ($g_{2,T,c} = g_{3,c} = 1.0$) at the same range point, $\varphi_{1,s}/\varphi_{1,c}$. This is the minimum value of h_2/h_1 that can be used and is also the point of maximum flow range (lowest $\varphi_{1,s}/\varphi_{1,c}$ possible) for the assumed values of $\varphi_{1,c}$, $\beta'_{1,c}$ and $(\overline{v}/V_{2,3})_s$. Also, for a given contraction of h_2/h_1 and $(\overline{v}/V_{2,3})_s$, a maximum pressure ratio at choke flow can be reached. This point is the point of stator-choke flow. The dashed line called maximum P_2/P_1 in figure 5(a) connects these points and shows how the choke-flow pressure ratio decreases as the range is increased ($\varphi_{1,s}/\varphi_{1,c}$ decreased). Figure 5(b) shows the results for the same design point with $(\overline{v}/V_{2,3})_s = 1.55$. Figure 6 shows the choke-flow maximum-pressure-ratio curves for both $(\overline{v}/V_{2,3})_s$ values for the design point at $\varphi_{1,c} = 0.65$, $\beta'_{1,c} = 45^\circ$. If a range of $\varphi_{1,s}/\varphi_{1,c} = 0.82$ is picked, the pressure ratio is 1.264 for a surface-velocity ratio of 1.75 and 1.178 for a velocity ratio of 1.55, the pressure rise being 50 percent higher for the case with $(\overline{v}/V_{2,3})_s = 1.75$.

Charts similar to those in figure 5 were drawn for each of the three channel angles of $\beta'_{1,c} = 30^\circ$, 45°, and 60° for various values of $\varphi_{1,c}$ but will not be shown since figure 5 shows typical results.

If consideration is limited to the class of compressor stages where $g_{2,T,c} = 1.0$ (maximum-pressure-ratio stages), only three independent variables remain. The relation among these three variables and other inflow parameters is shown graphically in figure 7 for $(\overline{v}/V_{2,3})_s = 1.75$. The results from figure 5(a) fall on one line with $\varphi_{1,c} = 0.65$ in the $\beta'_{1,c} = 45^\circ$ region, where the same limits that applied to figure 5(a) again occur; however, this time they are applied to numerous designs. The design limitation of $g_{3,c} = 1.0$ (choke at stator discharge) is encountered as the range is increased ($\varphi_{1,s}/\varphi_{1,c}$ decreased), which gives the lower boundary of the $\beta'_{1,c} = 45^\circ$ region. This design limitation $g_{3,c} = 1.0$ is reached as the flow range designed for the stage is increased, because the flow-range requirement of the stator is also increased; consequently, the stall-velocity ratio

$$\frac{V_{3,s}}{V_{2,s}} = \left(\frac{V_3}{\overline{v}_3}\right)_s \frac{\sin \beta_{2,s}}{\sin \beta_{2,c}}$$

must be raised by adjustment of h_3/h_2. The exit flow density ($g_{3,c}$) at choke flow then approaches 1.0 in accordance with the equation

$$g_{3,c} = g_{2,c}\left(\frac{g_3}{g_2}\right)_s \frac{\cos \beta_{2,c}}{\cos \beta_{2,s}}$$

and the additional condition of stator-throat choke ($g_{2,T,c} = 1.0$). The limit line ($g_{3,c} = 1.0$) in figure 7 is at a low inflow axial Mach number ($V_{1,z}/a_1^*$) because of the thick blades required for large flow range.

Another type of limit also occurs as a consequence of assuming that the stages are inlet stages with blades of maximum span and maximum h_1. If it is assumed that the design is stress-limited at the blade roots to attain a maximum flow by using a maximum inlet annulus area, the annulus-area ratio h_2/h_1 is limited to values of 1.0 or less. This annulus-area-ratio limit is encountered on the right of the $\beta'_{1,c} = 45^\circ$ region at high speeds when β'_2 is large. If high wheel speeds are used, the Mach number (V_2/a_2) into the stator can be controlled by discharging at large relative angles β'_2. The velocity W_2 is determined by the inflow conditions, and consequently h_2/h_1 must be increased as β'_2 is increased. The upper limit of the $\beta'_{1,c} = 45^\circ$ region is $\varphi_{1,s}/\varphi_{1,c} = 1.0$ (no flow range). The limit bounding the $\beta'_{1,c} = 45^\circ$ region on the left side would be some lower wheel speed limit. These limits apply to each of the $\beta'_{1,c}$ regions of figure 7.

Finally, the design is limited at low values of $\beta'_{1,c}$ because the assumed diffusion cannot, in these cases, be accomplished by turning without an annulus-area increase. Analytically stated, this condition is $h_2 \cos \beta'_2 < h_1$. This limit occurs in figure 7 as the upper limit of the $\beta'_{1,c} = 30^\circ$ region.

For any given rotor speed U_1/a_1^* and inflow Mach number $V_{1,z}/a_1^*$, a maximum-flow-range stage is obtained with a specific value of $\beta'_{1,c}$, which is determined by the condition $g_{3,c} = 1.0$; a higher channel angle $\beta'_{1,c}$ would give a stage with less flow range for the same rotor speed and inflow Mach number. A lower channel angle could not be achieved because of too small a blade span to handle the choke flow at the stator discharge.

Because of the overlapping area of the charts in figure 7 for the different values of $\beta'_{1,c}$, one pair of values of $V_{1,z}/a_1^*$ and U_1/a_1^* may be used with a variety of compressors, each one of which will differ from another by the angle $\beta'_{1,c}$. Each design, however, does have a maximum possible work input at choke flow.

Stage Flow Range

The maximum-flow-range stages, indicated by the curves for $g_{3,c} = 1.0$ in figure 7, exhibit a simple relation between the flow-range factor $\varphi_{1,s}/\varphi_{1,c}$ and the variables of $\varphi_{1,c}$, $\tan \beta'_{1,c}$ and $(\overline{v}/V_{2,3})_s$ as shown in figure 8. The importance of large surface diffusion is indicated by the increase in attainable flow range of compressor stages when $(\overline{v}/V_{2,3})_s$ is increased from 1.55 to 1.75.

The performance of the maximum-flow-range stages is shown in figure 9(a) for $(\overline{v}/V_{2,3})_s = 1.75$. The equivalent weight flow is estimated on the basis of an inlet radius ratio of 0.5, and the pitch radius is assumed to divide the annulus area into two equal parts. Maximum flow range varies little with channel angle $\beta'_{1,c}$, but variation with design speed is considerable and amounts to about 60 percent in the speeds from approximately 550 to 1050 feet per second. Pressure ratio and maximum flow depend primarily on channel angle $\beta'_{1,c}$ and only slightly on rotor speed.

The effect of reducing the blade-surface-diffusion ratios from 1.75 to 1.55 can be seen by comparing figures 9(a) and (b). A reduction in blade surface diffusion has the following effects: Maximum flow range is reduced about 27 percent, and higher flows and pressure ratios are obtained. If the higher velocity ratio of 1.75 were used with the same flow range as the maximum obtainable with a ratio of 1.55, the pressure ratio obtained would be higher than could be obtained with a surface-velocity ratio of 1.55.

Devices for increasing the over-all diffusion are therefore of great importance. For example, slotted blades or a rotor with two sequential sets of blades would permit some of these potential gains to be realized. Another such device is the increase of span between the rotor discharge and stator inlet, which can serve to reduce the axial velocity. As an example, one maximum-flow-range case was calculated for $\beta'_{1,c} = 45^\circ$, $\varphi_{1,c} = 0.65$ with $(\overline{v}/V_{2,3})_s = 1.75$. A value of $\varphi_{1,s}/\varphi_{1,c} = 0.723$ was obtained instead of the 0.752 obtained without increase in span; this is a 12-percent gain in maximum flow range for an area increase of 12 percent over a stage with the same inlet conditions designed for maximum flow range with a constant annulus area. The gain in

pressure ratio obtainable from high velocity-diffusion ratios is not worthwhile if the device requires additional space, because an additional stage could accomplish the same purpose; a gain in useful flow range is worthwhile since a reduction in flow range cannot be made up in subsequent stages.

Stage Stacking

When two compressor stages are stacked in series, the second stage must operate over a wider range of volume flow than the first because the discharge pressure of the first stage normally decreases with increasing mass flow. Consequently, the maximum-flow-range stages of figure 8 impose greater flow-range requirements on the second stage than can be attained.

If the compressor has only a few stages, say two or three, the flow range of the whole unit at normal speed may still provide a useful flexibility in operation. For such cases, it is of interest to consider a pair of stages in which the flow range of the first stage is reduced just sufficiently for the second stage to operate efficiently over the entire reduced flow range. The sacrifice in flow range of the first stage then permits a first-stage design with a pressure ratio increased over that for the maximum-flow-range stage.

A chart is shown in figure 10(a) for stages with flow ranges sufficiently reduced to permit a succeeding stage to operate over the entire flow range of the first stage. The effect of reducing the blade-surface-diffusion ratios from 1.75 to 1.55 can be seen by comparing figures 10(a) and (b).

Spanwise Variations

In the analysis, the blade row was treated as a two-dimensional cascade. Thus, limitations on the flow range and blade-row performance that resulted from end effects and spanwise variations were neglected. Consequently, the extreme range calculations and the maximum performance calculations based on the pitch section alone will be optimistic.

An estimate was made of spanwise variations of the blade shape, velocity, and velocity diffusion based on the assumption of an inlet radius ratio of 0.5 and constant tip radius by means of the equilibrium condition

$$\frac{dp}{dr} = \frac{V^2 \cos^2\theta}{r}$$

The blades were designed for simultaneous stall at hub, mean, and tip. The calculations were made only for cases of maximum pressure ratio ($g_{2,T,c} = 1.0$) and maximum flow range. In all cases designs were obtained with uniform stall conditions at the hub, mean, and tip sections. For operation at $\varphi = \varphi_{1,s}$ and $\varphi = \varphi_{1,c}$ at lower-than-design speed, all relative flow angles into the rotor are unchanged and the blade-surface-velocity diffusion decreases, so that the entire design-speed range is always available at the lower speeds. However, at design speed and choke flow, some blade section would be unable to accommodate the entire flow in the throat section without spanwise-flow adjustment. Consequently, the speeds estimated for choke of the mean section must be considered as somewhat optimistic when applied to a blade of large spanwise-flow variations and as more strictly applicable when applied to short-span blades.

4208

CONCLUDING REMARKS

CL-3

A method was developed for estimating the effect of blade flow range and compressor-stage flow range on other operating characteristics, such as choke-flow limit, pressure ratio, and operating speeds. Design limits to compressor-stage operation and design rotor speed were determined for the stage flow range. These results apply to a specific type of blade; however, they are believed applicable to most blade sections suitable for high-performance compressor designs.

The analysis of blade rows indicated that:

1. High Mach number designs necessarily have small flow ranges.

2. High blade-row flows per unit area are attained with low stagger and either low velocity diffusion or low flow range.

3. Maximum-flow-range blade rows are designed for critical discharge flow. The greatest flow range is attained at low values of Mach number, flow per unit area, and over-all velocity diffusion and at high surface-velocity diffusion.

4. For a compressor stage of maximum pressure ratio, assumption of values of choke flow, rotor speed, and channel stagger angle will determine the flow range, and also the stall and choke values for the flow directions, velocities, pressure ratio, and discharge Mach number. Maximum pressure ratio is attained when the stator throat is choked.

5. Blades designed to attain large surface-velocity diffusion may be used for either large pressure ratios or large flow range. The maximum flow range is nearly independent of channel angle $\beta'_{1,c}$.

6. A stage of maximum wheel speed for a given flow range is one of maximum relative discharge angle, and equal intake and discharge annulus areas.

7. A maximum-flow-range stage is attained when the discharge Mach number of the stage is critical. A particular channel angle $\beta'_{1,c}$ is required to attain the maximum flow range for a given rotor speed and airflow.

Lewis Flight Propulsion Laboratory
National Advisory Committee for Aeronautics
Cleveland, Ohio, February 28, 1958.

[redacted]

APPENDIX A

SYMBOLS

A	channel frontal area
a	local velocity of sound
a^*	critical velocity of sound
b	distance BA along suction surface (fig. 1)
D	over-all diffusion
G	$\equiv \frac{\rho W}{\rho^* a^*}$ for rotor
g	$\equiv \frac{\rho V}{\rho^* a^*}$ for stator
h	annulus area per blade channel
M	Mach number, ratio of local velocity to local velocity of sound
M^*	critical Mach number, ratio of local velocity to critical velocity of sound
ΔM	$= \frac{M_A^* - M_B^*}{M_A^* + M_B^*}$
P	total pressure
p	static pressure
$\overline{R}$	average radius of curvature on the suction surface along b (fig. 1)
r	radius
s	blade spacing (fig. 1)
t	throat distance (fig. 1)
U	mean wheel speed

V	mean absolute flow velocity
v	surface velocity
$\overline{v}$	average surface velocity
W	mean relative flow velocity
$\overline{w}$	average surface velocity on the rotor suction surface b
x	distance along airfoil surface
β	absolute blade angle
β'	relative blade angle
γ	ratio of specific heats
θ	inflow air angle
ρ	density
ρ^*	critical density
φ	flow coefficient = $\frac{V \cos \theta}{U}$

Subscripts:

A	condition at point A on suction surface (fig. 1)
a	stagnation condition
B	condition at point B on pressure surface (fig. 1)
c	choke condition
m	maximum
p	condition when air is tangent to pressure surface
s	stall condition
T	throat
z	axial component
1	rotor entrance

[redacted]

2 rotor exit

3 stator exit

APPENDIX B

MAXIMUM INFLOW TO A CASCADE

At maximum inflow conditions, the velocity in the throat of a cascade of blades is nearly sonic; the flow density may then be approximated by

$$\frac{\overline{\rho V}}{\rho^* a^*} = 1 - \frac{\gamma + 1}{2}\left(1 - \frac{V}{a^*}\right)^2$$

If a linear variation of V/a^* across the channel is assumed, the mean flow density is

$$\frac{\overline{\rho V}}{\rho^* a^*} = \frac{1}{t}\int_0^t \left(\frac{\rho V}{\rho^* a^*}\right) dt = 1 - \frac{\gamma + 1}{6}\left[3(1 - \overline{M})^2 + \overline{M}^2\,\Delta M^2\right]$$

where $\overline{M} = (V_A + V_B)/2a^*$ and $\Delta M \equiv (V_A - V_B)/(V_A + V_B)$.

If ΔM is assumed independent of $\overline{M}$, then the maximum flow density is obtained when $\overline{M} = 1/(1 + \Delta M^2/3)$ and its value is

$$\left(\frac{\overline{\rho V}}{\rho^* a^*}\right)_m = 1 - \frac{\gamma + 1}{6}\Delta M^2 \frac{1 + \Delta M^2}{\left(1 + \frac{\Delta M^2}{3}\right)^2} \approx 1 - \frac{\gamma + 1}{6}\Delta M^2$$

The effect of cross-channel velocity variations is very slight; when $V_A/V_B = 1.5$, the average choking flow density is reduced only 1.6 percent. On a one-dimensional basis, the flow upstream of the cascade is then

$$\frac{\rho_1 V_1}{\rho^* a^*}\, s \cos\theta_1 = \left(\frac{\overline{\rho V}}{\rho^* a^*}\right)_T t$$

where t is the throat size. This equation determines the relation between the upstream critical Mach number M_1^*, and the angle θ_1 for a given throat area when the throat flow is choked. The result is sometimes given in the form:

$$\frac{A_T}{A_1} = \frac{t}{s\cos\theta_1} = \frac{\rho_1 V_1/\rho^* a^*}{(\overline{\rho V}/\rho^* a^*)_T} = \frac{\rho_1 V_1}{\rho^* a^*}$$

[redacted]

Since $\rho_1 V_1/\rho^* a^*$ is a function of M_1, the inflow Mach number may be plotted as a function of A_T/A_1 for any actual cascade. In reference 8 agreement with theory is shown as good for $A_T/A_1 \leq 0.97$. Above this value, A_1 is decreased by increasing the angle of attack; consequently, the boundary-layer thickness is increased with increasing A_T/A_1 until separation is reached. Thus, the experimental flow capacity is lower than the estimated value by an amount that increases with A_T/A_1, M_1, or β_1; with very thick blades this effect is accentuated by the very high angles of attack required. The data of reference 9 show the same agreement. The cascade data of reference 10 have only one datum in the range $A_T/A_1 < 1.0$, where the flow is 3 percent low; this amount is explained by the estimate of throat variation of the Mach number. For the special family of airfoils selected, the throat area may be estimated by using the circular-arc approximation for the exposed portion of the suction surface. The result is:

$$\frac{t}{s \cos \theta_1} = \frac{\cos\left(\frac{\beta_s + \beta_p}{2}\right)}{\cos \theta_1 \cos\left(\frac{\beta_s - \beta_p}{2}\right)}$$

If, in application, the formula is to be used with $t/(s \cos \theta_1) < 1$, then $\theta_1 < (\beta_s + \beta_p)/2$ must be used (the inflow angle must be less than the inlet camber-line angle). An integral across the throat yields:

$$\Delta M \equiv \frac{M_A^* - M_B^*}{M_A^* + M_B^*} \cong \frac{t}{2\bar{R}} = \frac{1}{2}\left[\frac{\sin \beta_s}{\sin \beta_p} - 1\right]$$

which, with

$$\frac{\rho_1 V_1}{\rho^* a^*} = \frac{(1 - 0.4\ \Delta M^2)}{\cos \theta_1} \frac{\cos\left(\frac{\beta_s + \beta_p}{2}\right)}{\cos\left(\frac{\beta_s - \beta_p}{2}\right)}$$

determines the maximum flow in the cascade.

This result applies strictly to two-dimensional full-flowing channels.

REFERENCES

1. Weinig, F.: Die Strömung um die Schaufeln von Turbomaschinen. Johann Ambrosius Barth (Leipzig), 1935.

2. Loftin, Laurence K., Jr., and von Doenhoff, Albert E.: Exploratory Investigation at High and Low Subsonic Mach Numbers of Two Experimental 6-Percent-Thick Airfoil Sections Designed to Have High Maximum Lift Coefficients. NACA RM L51F06, 1951.

3. Herrig, L. Joseph, Emery, James C., and Erwin, John R.: Systematic Two-Dimensional Cascade Tests of NACA 65-Series Compressor Blades at Low Speeds. NACA RM L51G31, 1951.

4. Westphal, Willard R., and Godwin, William R.: Comparison of NACA 65-Series Compressor-Blade Pressure Distributions and Performance in a Rotor and in Cascade. NACA RM L51H20, 1951.

5. Savage, Melvyn: Analysis of Aerodynamic Blade-Loading-Limit Parameters for NACA 65-$(C_{l_0} A_{10})10$ Compressor-Blade Sections at Low Speeds. NACA RM L54L02a, 1955.

6. Andrews, S. J.: Tests Related to the Effect of Profile Shape and Camber Line on Compressor Cascade Performance. R. & M. 2743, British ARC, 1949.

7. Howell, A. R.: A Note on Compressor Base Aerofoils C.1, C.2, C.3, C.4, C.5, and Aerofoils Made up of Circular Arcs. Memo. M.1011, Power Jets Ltd., Sept. 1944.

8. Andrews, S. J., Andrews, Patricia M., and Baines, Margaret: A Comparison Between Two Compressor Cascades Using C.4 Profile on Parabolic and Circular Arc Camber Lines. Memo. No. M.6, British NGTE, Sept. 1946.

9. Bailey, W., and Jefferson, J. L.: Compressibility Effects on Cascades of Low Cambered Compressor Blades. Rep. E.3972, British RAE, May 1943.

10. Howell, A. R.: The Present Basis of Axial Flow Compressor Design. Pt. 1 - Cascade Theory and Performance. R. & M. 2095, British ARC, 1942.

[redacted]

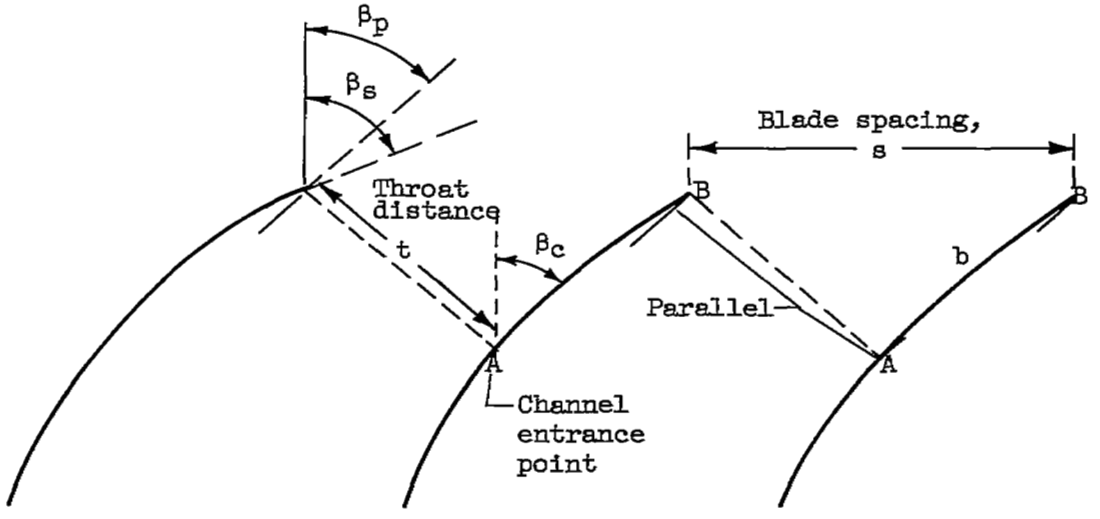

Figure 1. - Type of cascade investigated.

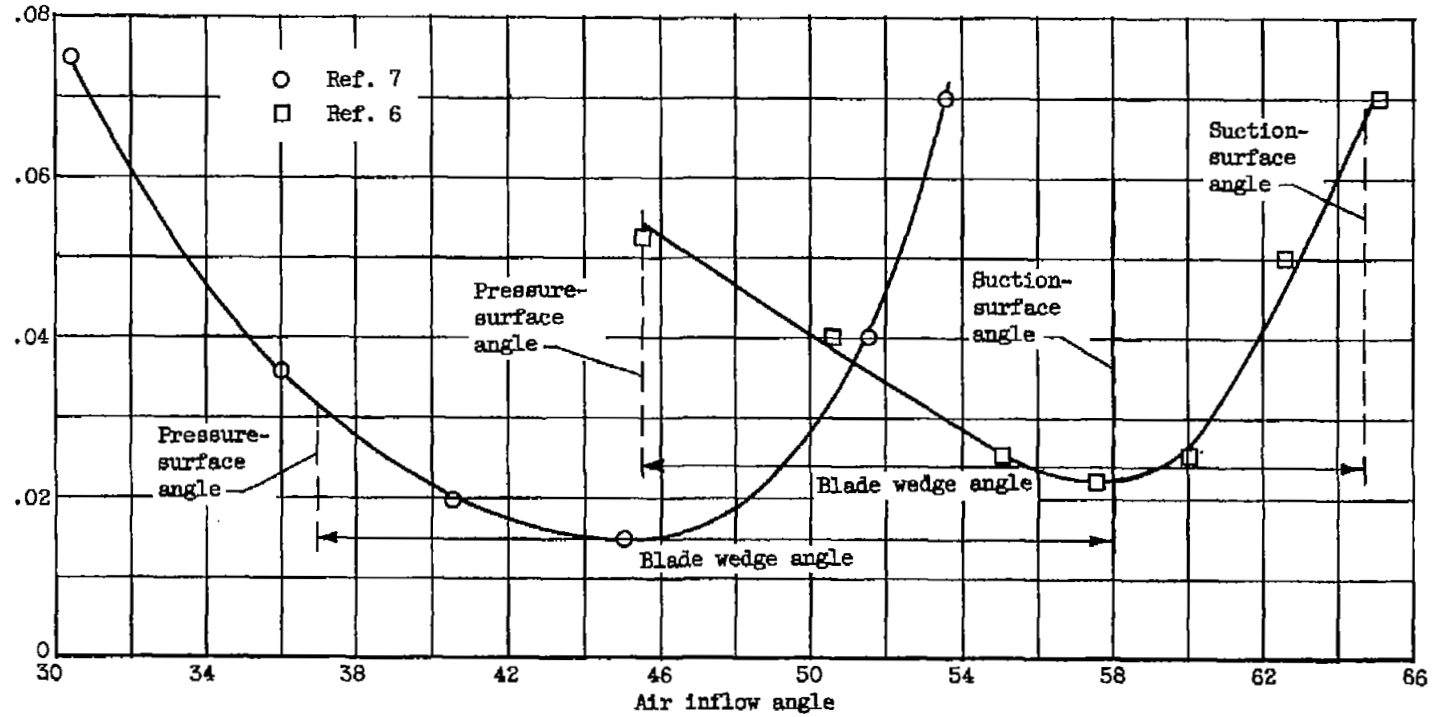

Figure 2. - Low-speed loss data from cascades.

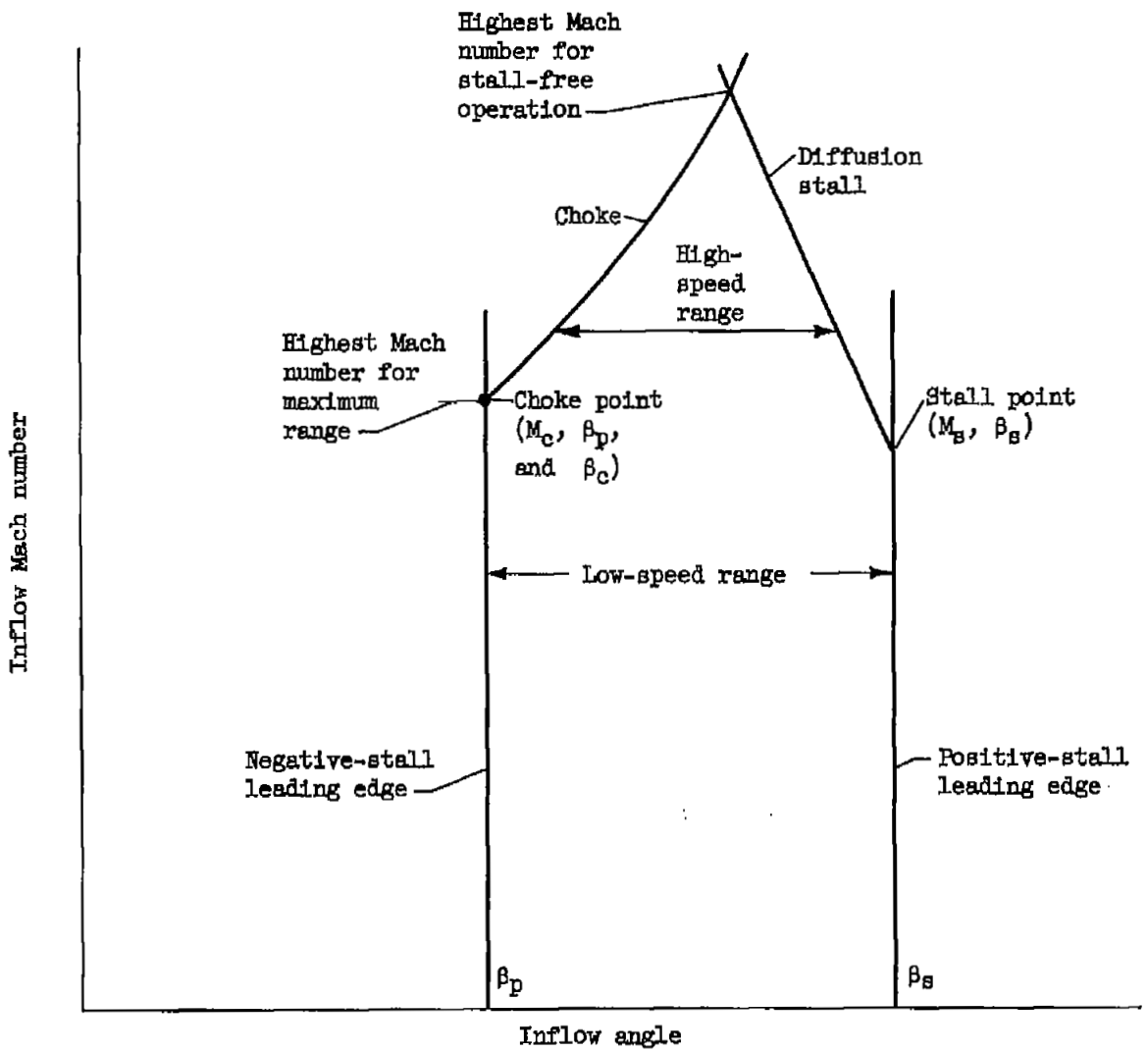

Figure 3. - Limits on operating range of blade row.

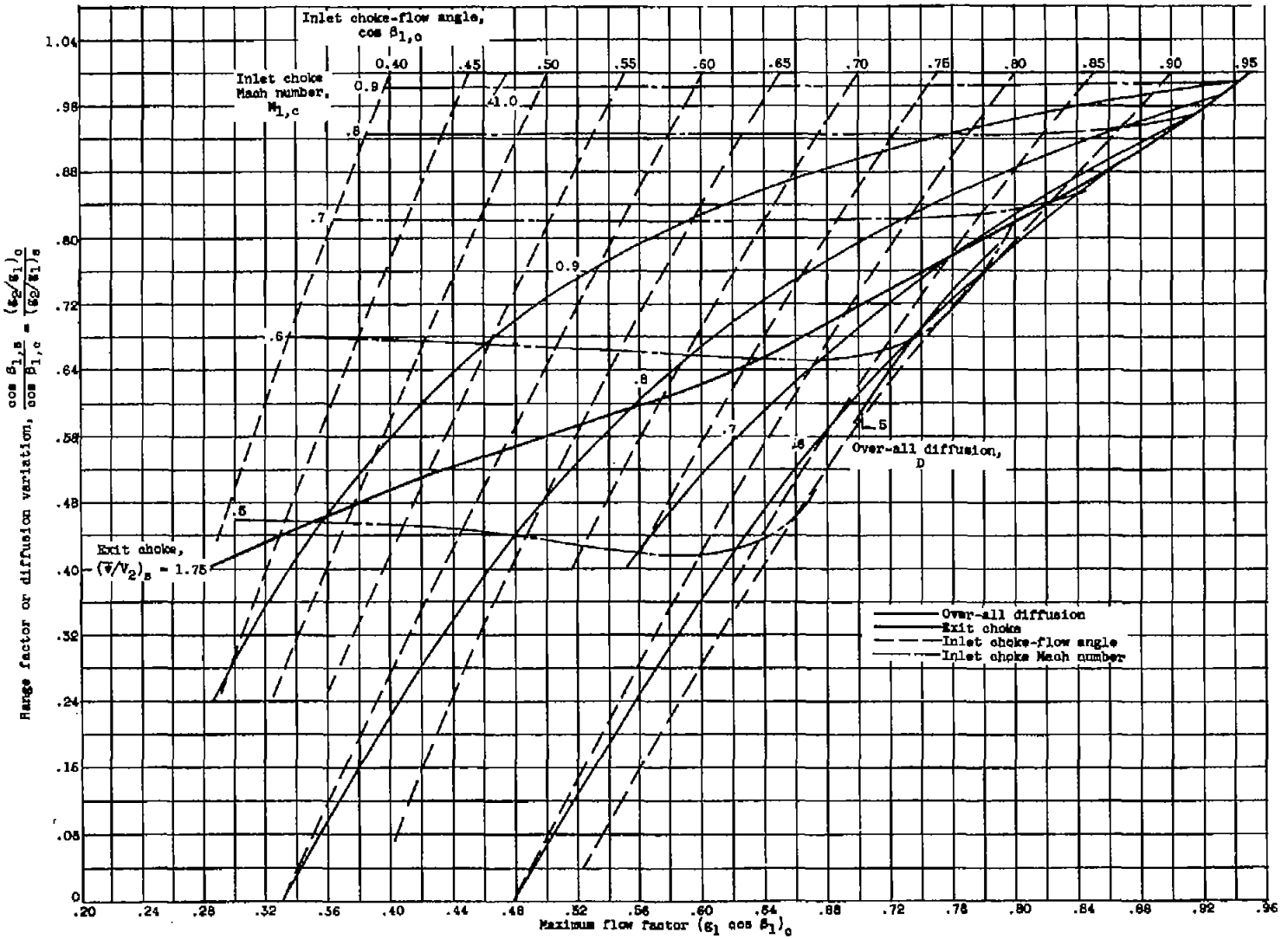

Figure 4. - Performance of single blade rows. $(\bar{v}/V_2)_D = \frac{\bar{v}}{V_2} \frac{\sin \beta_c}{\sin \beta_s} = (V_1/V_2)_s$.

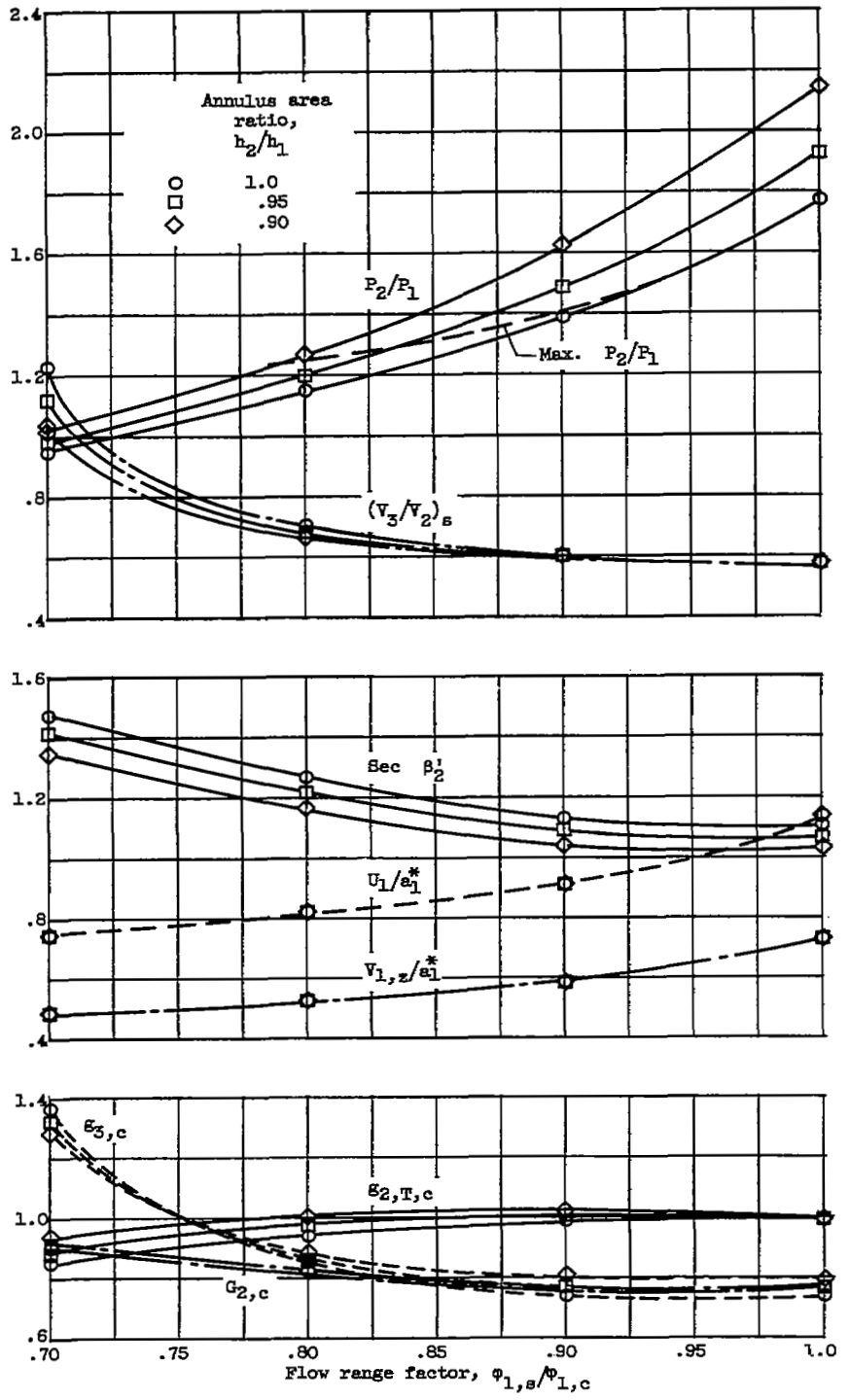

(a) Surface velocity ratio, 1.75.

Figure 5. - Performance for design point at choke flow coefficient of 0.65, relative flow angle of 45°, with rotor throat choke.

[redacted]

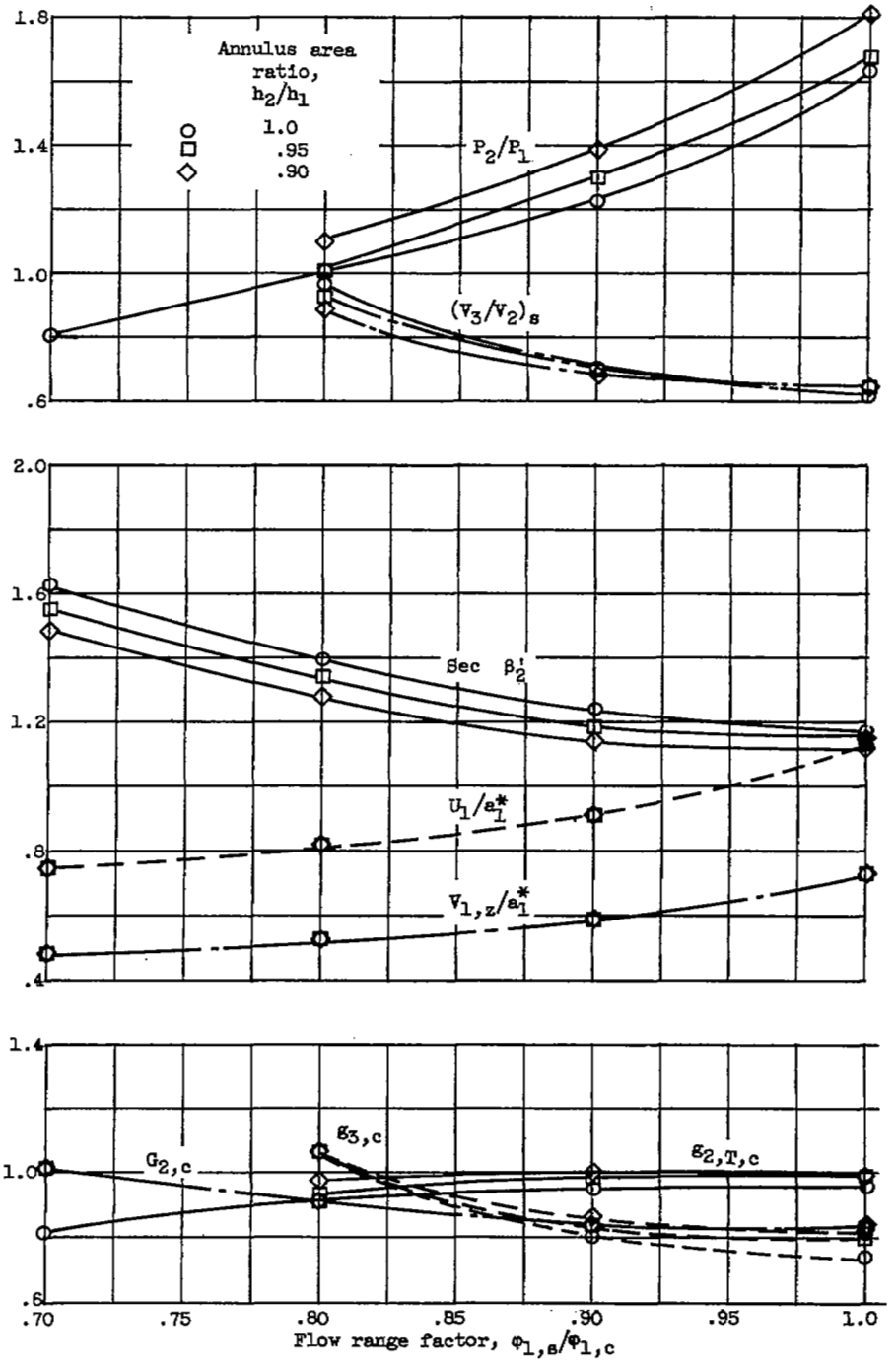

(b) Surface velocity ratio, 1.55.

Figure 5. - Concluded. Performance for design point at choke flow coefficient of 0.65, relative flow angle of 45°, with rotor throat choke.

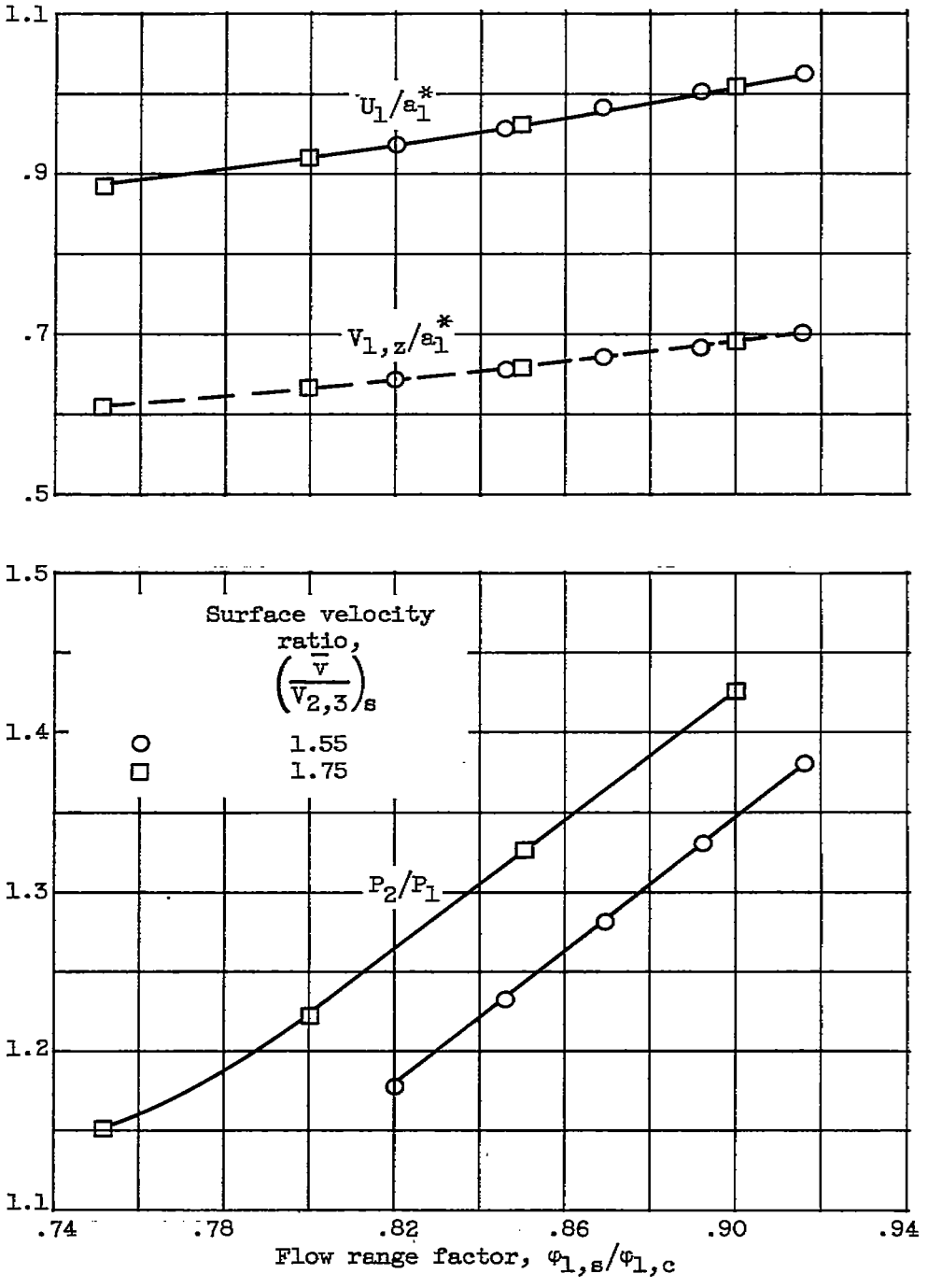

Figure 6. - Maximum-pressure-ratio stages for design point at choke flow coefficient of 0.65 and relative flow angle of 45°.

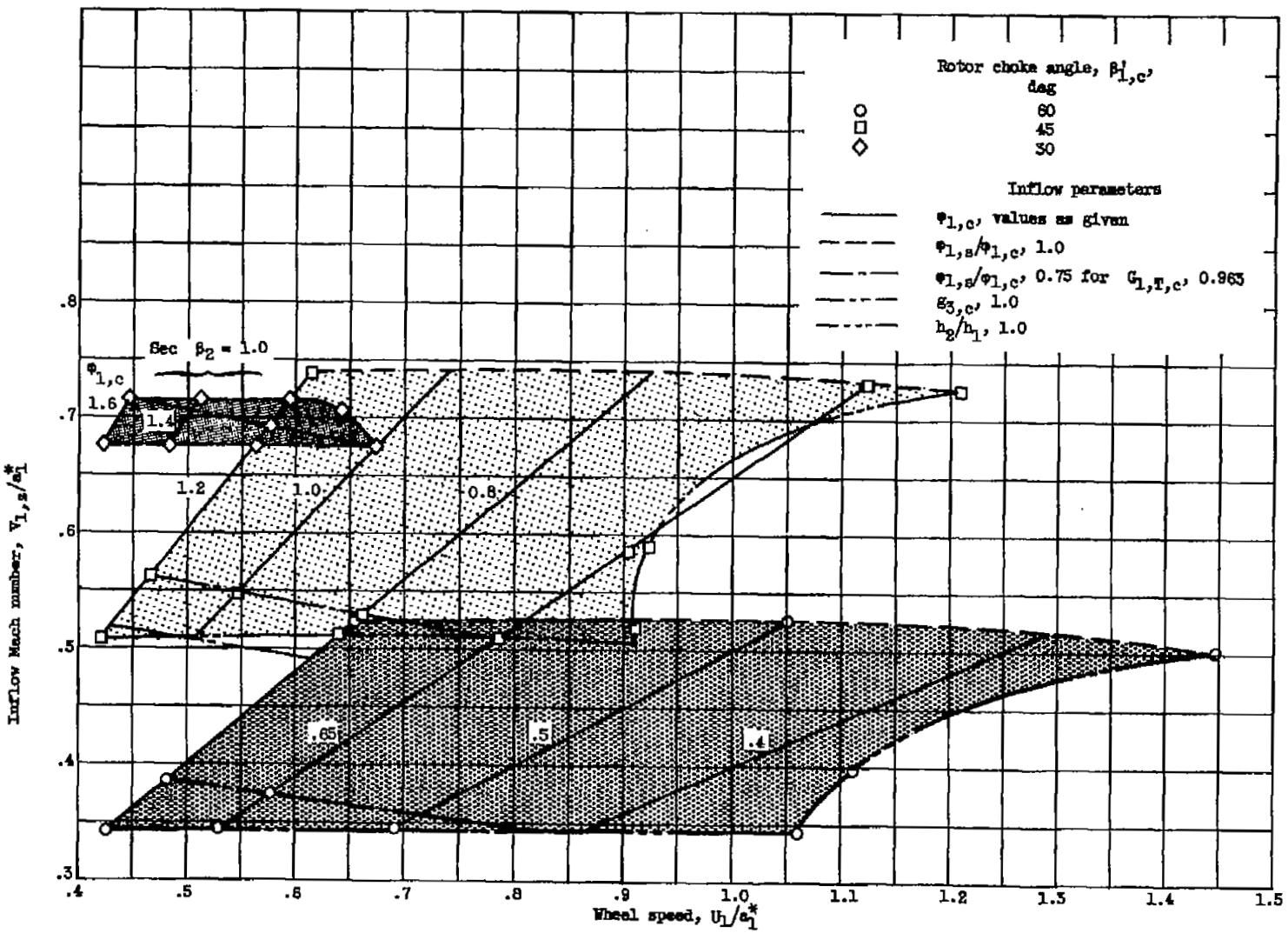

Figure 7. - Relations among choke flow coefficient, stall flow coefficient, relative flow angle, and other inflow parameters with rotor throat choke and a surface velocity ratio of 1.75.

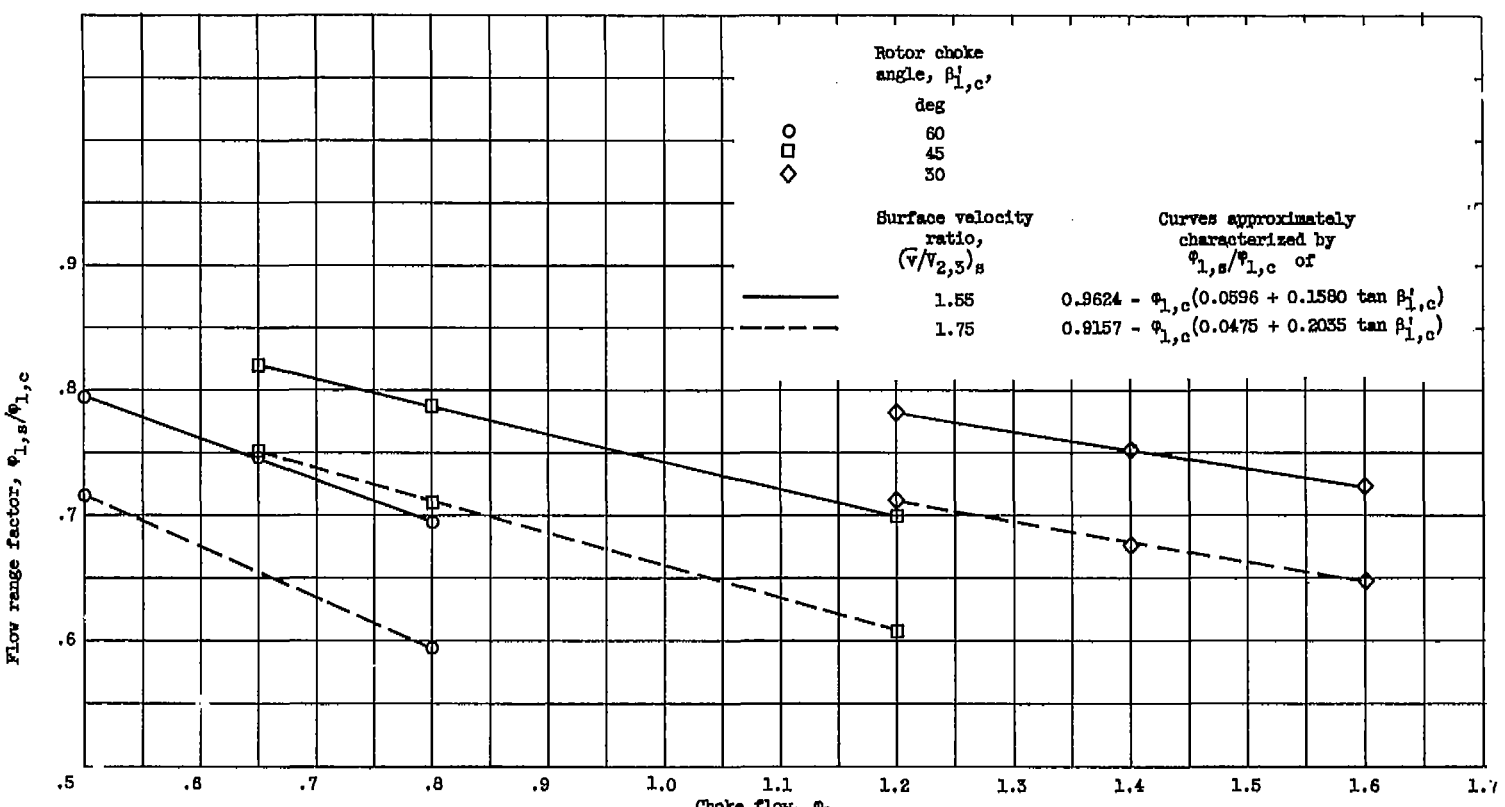

Figure 8. - Maximum range for various values of choke flow coefficient and relative flow angles with rotor throat choke and stator throat and exit choke.

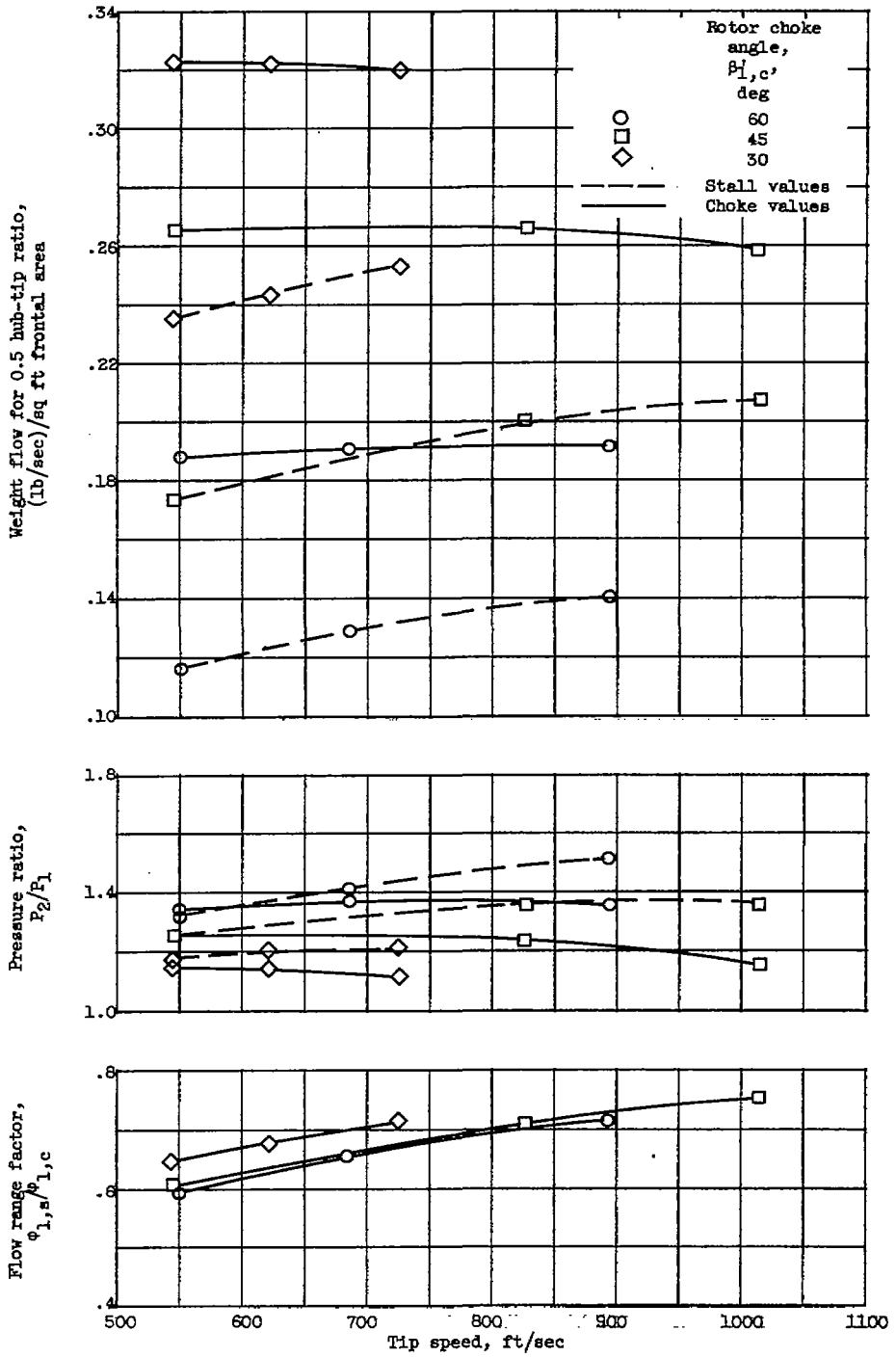

(a) Surface velocity ratio, 1.75.

Figure 9. - Performance characteristics for maximum-flow-range stages with rotor throat choke.

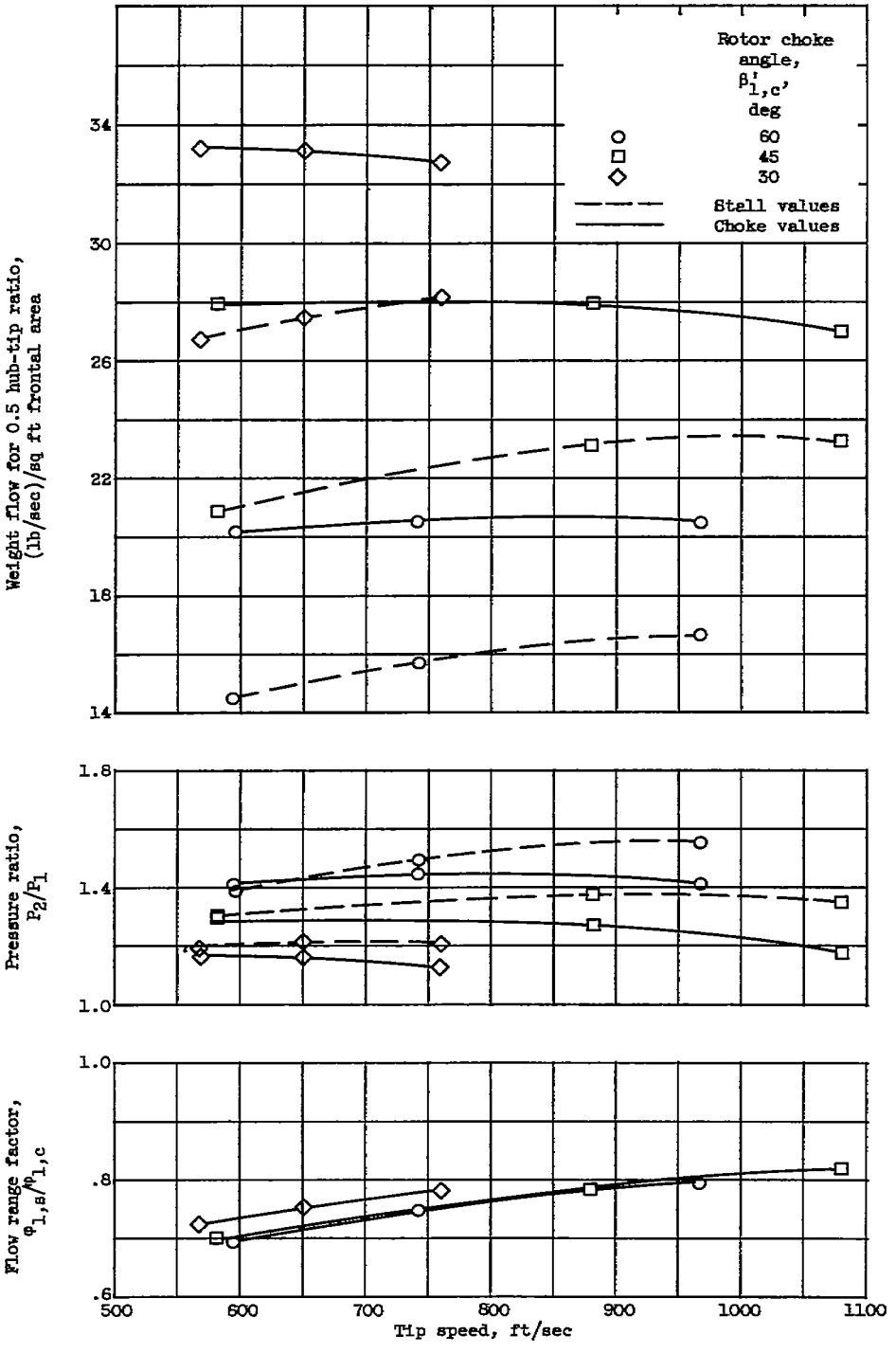

(b) Surface velocity ratio, 1.55.

Figure 9. - Concluded. Performance characteristics for maximum-flow-range stages with rotor throat choke.

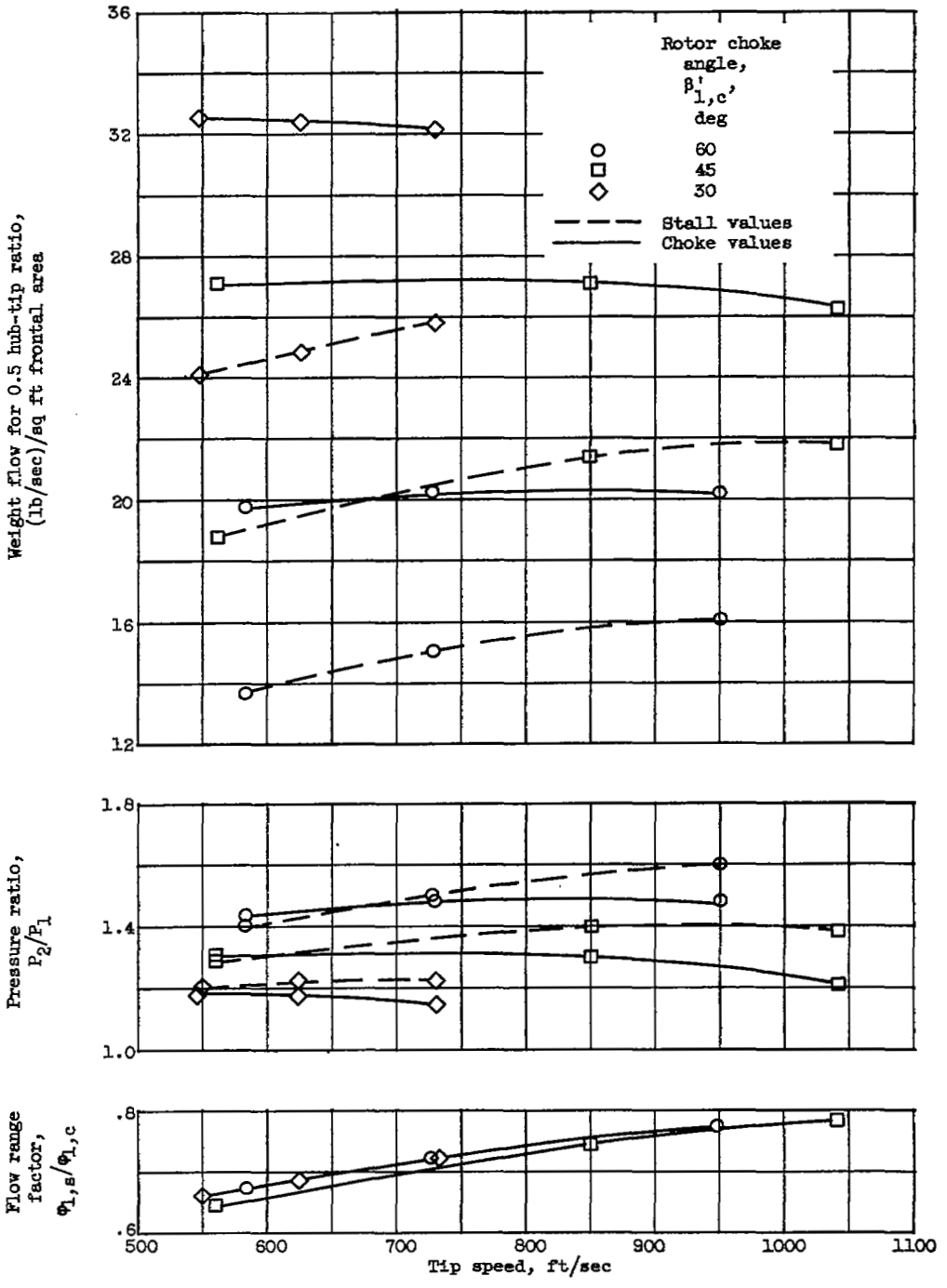

(a) Surface velocity ratio, 1.75.

Figure 10. - Performance characteristics for repeatable stages with rotor throat choke.

[redacted]

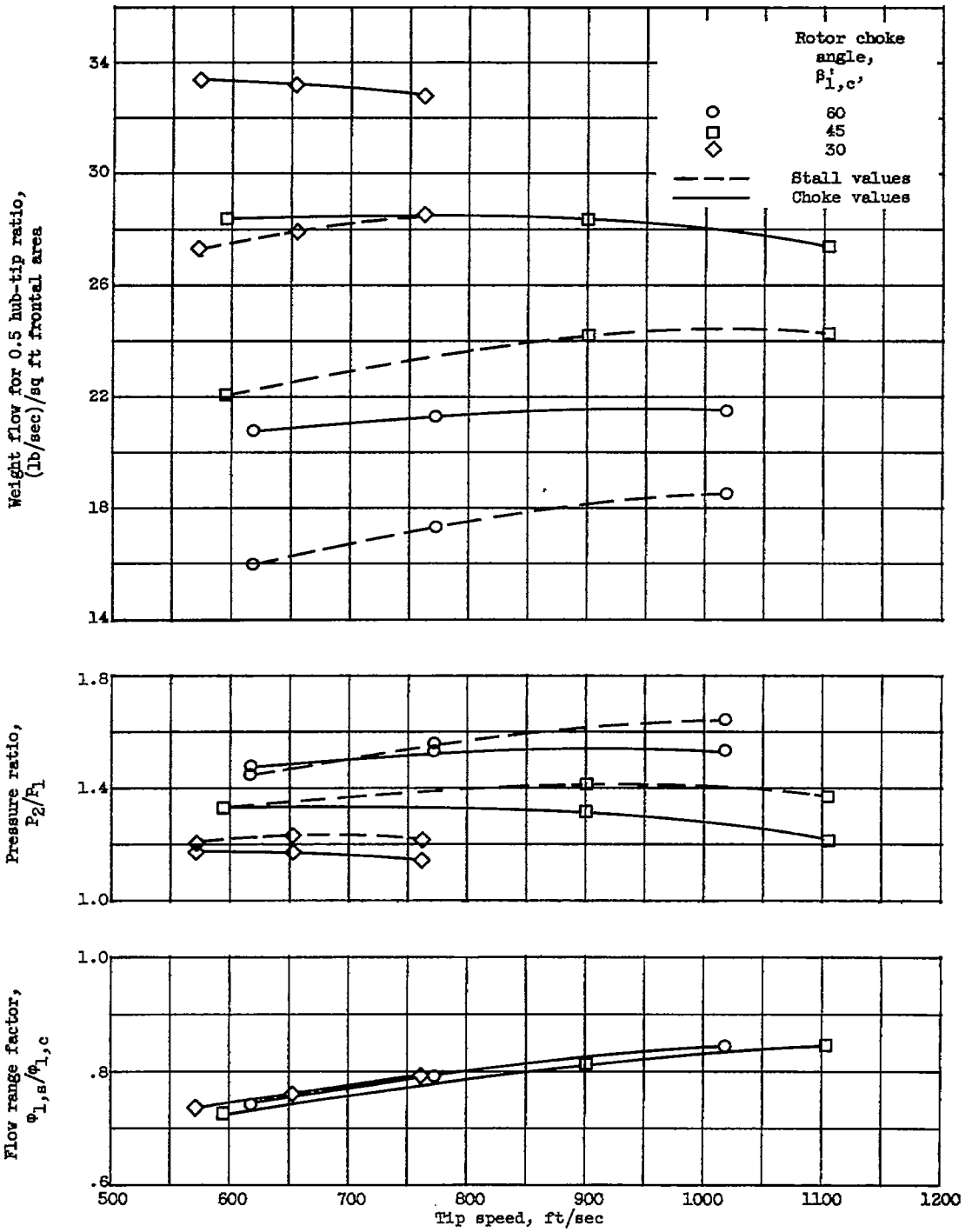

(b) Surface velocity ratio, 1.55.

Figure 10. - Concluded. Performance characteristics for repeatable stages with rotor throat choke.

[redacted]